RESEARCH ARTICLE
doi: 10.2306/scienceasia1513-1874.2026.044

ScienceAsia 52 (2): 2026: ID 2026044: **1–11**

Overexpression of ubiquitin specific protease 25 suppresses osteoclastogenesis and alleviates bone loss in OVX mice

Qunhu Zhang[a,†], Huanhuan Chen[a,†], Shiyuan Yin[a], Yu Wang[a], Chengjuan Wang[a], Ce Shi[b,*], Chaoming Huang[a,*]

[a] Jiangsu Province (Suqian) Hospital, Suqian, Jiangsu 223800 China
[b] Suqian People's Hospital of Nanjing Drum-Tower Hospital Group, Suqian, Jiangsu 223800 China

*Corresponding authors, e-mail: shice99@126.com, huangao2019@163.com
† These authors contributed equally to this work.

Received 15 Jan 2025, Accepted 27 Apr 2026
Available online 18 May 2026

ABSTRACT: Ubiquitin specific protease 25 (USP25), a deubiquitinase, has been associated with inflammation, cancer, and immune response. However, the effect of USP25 on bone metabolism in postmenopausal osteoporosis (PMOP) is still unclear. Here, we examined the role of USP25 in the regulation of bone resorption and osteoclastogenesis in PMOP. The expression of USP25 was assessed in patients with PMOP and ovariectomy (OVX) mice. The role of USP25 on osteoclastogenesis was analyzed using osteoclastogenesis and bone resorption assays. The effect of USP25 inhibition was evaluated in a OVX mice model. The mechanism by which USP25 regulates osteoclastogenesis and bone resorption was explored through a series of *in vitro* studies. USP25 was downregulated in OVX mice and PMOP patients. USP25 suppressed osteoclastogenesis and bone resorption *in vitro*, and it inhibited the expression of osteoclast-related genes. USP25 regulated osteoclastogenesis by promoting tumor necrosis factor receptor-associated factor 6 (TRAF6) deubiquitination. Moreover, AZ1, a selective small molecule blocker of USP25, could exacerbate pathological bone loss in OVX mice. In conclusion, these data unequivocally suggest that USP25 could suppress osteoclast differentiation and impede bone absorption by restraining TRAF6 polyubiquitination. USP25 overexpression could effectively alleviate pathological bone loss in OVX mice. Therefore, USP25 may be used as a new target for the treatment of bone loss in PMOP.

KEYWORDS: postmenopausal osteoporosis, osteoclast, USP25, TRAF6, deubiquitination

INTRODUCTION

Bone homeostasis is maintained by the equilibrium between bone formation by osteoblasts and bone resorption by osteoclasts [1]. Over-differentiation and hyperfunction of osteoclasts can result in osteoporosis (OP), rheumatoid arthritis, and Paget's disease [2]. Osteoporosis is a metabolic bone disease characterized by low bone density and structural changes, resulting in heightened bone fragility and an elevated risk of fractures [3]. Postmenopausal osteoporosis (PMOP) is the most prevalent type of OP, and it is caused by rapid bone depletion induced by estrogen deficiency following menopause [4]. Bone mineral density (BMD), as measured by dual X-ray absorptiometry, serves as a crucial diagnostic tool for OP. As per the guidelines set by the WHO, OP is defined by a T-score $\leqslant -2.5$, while a T-score $\geqslant -1.0$ indicates normal bone mass [5]. Roughly 50% of postmenopausal women will suffer from fragility fractures, resulting in pain, disability, and diminished quality of life [6]. To date, almost all strategies for preventing and treating OP have not achieved satisfactory results [7].

The ubiquitin-proteasome system is the principal pathway for intracellular protein degradation that can regulate a large number of cellular life activities, including cell cycle, transcriptional regulation, immune response, DNA repair, and signal transduction [8]. The binding of ubiquitin to the target protein is continuously catalyzed by ubiquitin activation enzyme E1, ubiquitin coupling enzyme E2, and ubiquitin-protein ligase E3, leading to the establishment of polyubiquitin chains on the target protein [9]. Subsequently, the target protein is degraded by proteasomes capable of recognizing polyubiquitin chains [10]. Ubiquitin specific protease 25 (USP25) is a deubiquitinase that can negatively regulate the ubiquinization of proteins by removing the ubiquitin connected to the proteins [11]. USP25 exhibits the ability to hydrolyze K48- and K63-linked polyubiquitin chains (K63-Ub), serving as targets for a range of post-translational modifications, including ubiquitination, phosphorylation, and SUMOylation [12]. Generally, USP25 has been related with cancer, inflammation, and immune response [13]. Deficiency in USP25 activates the TBK1–NF-κB pathway, resulting in heightened expression of inflammatory cytokines in bone marrow–derived macrophages (BMDMs) that can serve as precursor cells for osteoclasts, and ultimately exacerbating L-arginine-induced acute pancreatitis [14]. In acute kidney injury, the USP25-PKM2 axis of acid glycolysis positively regulates M1 like polarization of RAW264.7 and primary BMDMs [15]. However, it remains unclear whether USP25 influences osteoclastogenesis in PMOP. Moreover, AZ1

is one of the three benzylaminoethanol derivatives (AZ1, AZ2, and AZ4), which has been identified as an effective inhibitor of USP25 and has been applied in many *in vivo* studies involving USP25, such as cancer, inflammation, and Alzheimer's disease [16]. The palmar fissure of the thumb represents the binding site of AZ1 in USP25 [17].

Previous studies showed that tumor necrosis factor (TNF) receptor-associated factor 6 (TRAF6) plays a crucial role in the signal transduction of receptor activator of nuclear factor-κB (RANK)-RANK ligand (RANKL) signal pathway that induces osteoclastogenesis [18]. TRAF6 is a RING-type E3 that catalyzes K63-Ub using the Ubc13/Uev1A complex as the E2 [19]. After RANK activation, TRAF6 is recruited into upstream signaling complexes, and K63-Ub is conjugated to transforming growth factor-β-activated kinase 1 (TAK1) binding protein 2 (TAB2) or TAB3 by TRAF6, in turn inducing a conformational change that activates TAK1 [20, 21]. Continuing, downstream mitogen activated protein kinase (MAPK) and inhibitor of nuclear factor κB kinase (IKK) are activated, finally leading to the activation of activator protein 1 (AP-1) and nuclear factor κB (NF-κB) [22].

Herein, we found that USP25 could suppress osteoclastogenesis, and abate the bone resorption ability of osteoclasts. USP25 overexpression could effectively impede the RANKL-RANK-TRAF6 signaling, and prevent ovariectomy (OVX) mice from bone loss. AZ1 exacerbates pathological bone loss in OVX mice.

MATERIALS AND METHODS

Reagents

The cell-culture reagents were provided by Gibco BRL (New York, USA). Mouse RANKL recombinant protein (cat. no. 315-11) was obtained from PeproTech (Rocky Hill, USA). Recombinant mouse MCSF protein (ab129146), and the following antibodies: USP25 (ab246948), TRAF6 (ab137452), TAK1 (ab109526), p-TAK1 (ab109404), p65 (ab32536), p-p65 (ab76302), JNK (ab179461), p-JNK (ab124956), K63-Ub (ab179434), GAPDH (ab181602), β-actin (ab213262) were obtained from Abcam (Cambridge, England). NFATc1 (sc-7294) antibody was obtained from Santa Cruz Biotechnology (Santa Cruz, USA). AZ1 (cat. no. 2165322-94-9) was obtained from TargetMol (Boston, USA).

Cell culture and osteoclast differentiation

RAW264.7 cells were kindly provided by Cell Bank, Chinese Academy of Sciences (Shanghai, China). Bone marrow monocytes (BMMs) were collected from 6-week-old female C57BL/6 mice by flushing out the marrow cavity of femur and tibia. Cell culture and osteoclast differentiation were performed as previously described [23].

USP25 shRNA and overexpression (OE) USP25

Lentivirus with shRNA targeting murine USP25 (cat. no. 115658-1, 115659-1, Genechem, Shanghai, China) were added for 48 h. To establish stable cell lines, cells infected with the lentiviral USP25 shRNA were selected using puromycin (5.0 μg/ml). The culture medium was substituted once with fresh medium containing puromycin every 2 days. Typically, resistant colonies were successfully formed after 7 to 8 days. Control cells were infected with scramble nonsense shRNA (scr-shRNA) lentiviral GFP. Cells overexpressing USP25 (cat. no. 85230-1, Genechem) were obtained by following the same procedure.

Tartrate-resistant acid phosphatase (TRAP) staining assay

The TRAP staining assay was performed as previously described [23]. The following reagents were used: TRAP Kits (cat. no. 387A, Sigma-Aldrich, St. Louis, USA), EDTA (cat. no. E1171, Solarbio, Beijing, China), Optimal Cutting Temperature (OCT) compound (cat. no. 4583, Sakura, Torrance, USA). Pictures were taken using a Nikon Eclipse Ti2-e microscope (Nikon, Tokyo, Japan). Image analysis was performed using Image J v1.8.0 software.

Quantitative PCR (q-PCR)

qPCR was conducted with the ChamQ Universal SYBR qPCR Master Mix (cat. no. Q711-02, Vazyme, Nanjing, China) as previously described [23]. At 8 weeks after OVX, proximal femurs of mouse were taken from the left hind limbs. Total RNA was isolated using an RNA-Quick Purification Kit (cat. no. RN001, ES Science, Shanghai, China). Primer (Sangon Biotech, Shanghai, China) sequences are as followings: *usp25* (5′-CAGAAGCACCAGCAGACATTT-3′, 5′-TGGCATTCTTTGCAGTGAGGA-3′), *β-actin* (5′-CTAGTACGTTGCTATCCAGGC-3′, 5′-CTCCTTAATGTCACGCACGAT-3′), *ctsk* (5′-CTCGGCGTTTAATTTGGGAGA-3′, 5′-TCGAGAGGGAGGTATTCTGAG-3′), *acp5* (5′-CACTCCCACCCTGAGATTTGT-3′, 5′-CCCCAGAGACATGATGAAGTC-3′), *nfatc1* (5′-GGAGAGTCCGAGAATCGAGAT-3′, 5′-TTGCAGCTAGGAAGTACGTCT-3′).

Bone resorption assay

The bone resorption assay was conducted as previously described [23]. In brief, cells were seeded at a density of 10,000 (RAW264.7) or 20,000 (BMMs) per well in Corning Osteo Assay Surface Plate (cat. no. 3987, Corning, USA), and stimulated with RANKL (50 ng/ml) for 7 days, either in the absence of (RAW264.7) or in the presence of (BMM) macrophage colony stimulating factor (M-CSF) (30 ng/ml). Then, the conditioned medium was removed from each well. And, the wells were treated with 5% sodium hypochlorite to eliminate the cells. Pictures were captured

using a Nikon Eclipse Ti2-e microscope (Nikon). Image analysis was performed using Image J v1.8.0 software.

Western blot analysis

RAW264.7 cells were plated onto 6-well plate at a density of 50,000 or 5×10^5 cells per well and stimulated with cytokines of the indicated concentration for 2 days or the designated duration. For the phosphorylation assay, cells were subjected to starvation for 8 h and then pretreated with PBS for 40 min. At 8 weeks after OVX, proximal femur of mice was excised from the right hind limb. According to the Declaration of Helsinki, human bone samples of femoral neck were obtained from patients who underwent total hip arthroplasty (THA) due to femoral neck fracture (5 cases in control group with $T \geqslant -1.0$ and 5 cases in PMOP group with $T \leqslant -2.5$). Subsequently, the total proteins were isolated. Assays were conducted as previously stated [23] using following antibodies: USP25 (1:500), NFATc1 (1:500), TRAF6 (1:1000), TAK1 (1:1000), p-TAK1 (1:1000), p-p65 (1:1000), p65 (1:2000), JNK (1:2000), p-JNK (1:1000), GAPDH (1:5000), β-actin (1:5000) and K63-Ub (1:1000).

Immunohistochemistry (IHC)

The proximal femur of mice was fixed using 4% paraformaldehyde for 24 h, followed by decalcification using EDTA at 4 °C for 2 weeks. Decalcified samples were embedded into OCT and sectioned (5 μm thick) with cryostat. The sections were incubated overnight at 4 °C with USP25 (1:100) primary antibodies. A secondary biotinylated goat anti-rabbit antibody (1:1000) was added for 30 min, followed by detection of immunoactivity using a horseradish peroxidase-streptavidin detection system. The sections were assessed in a blinded manner by two independent histology researchers.

Coimmunoprecipitation (Co-IP)

The experimental method of Co-IP was described previously [24]. Briefly, the anti-TRAF6 antibody was added to the cell lysates and incubated overnight at 4 °C. Subsequently, pierce protein A/G magnetic beads (cat. no. 88804, Thermo Scientific, Waltham, USA) were submerged in the lysates. The TRAF6-immunoprecipitated proteins were captured and detected through Western blot analysis.

OVX mice

8-week-old Female C57BL/6 mice were anesthetized with sodium pentobarbital (30 mg/kg; i.p.), and subjected to OVX. The sham surgery group mice were only removed some adipose tissue around the ovaries. Two weeks after surgery, C57BL/6 mice were intraperitoneally injected with AZ1 (20 mg/kg in 0.5 ml PBS) or PBS (0.5 ml) daily for 6 weeks. Mice were euthanized by injection with pentobarbital (30 mg/kg; i.p.), followed by cervical dislocation. Heartbeat and breathing were checked to ensure successful euthanasia. Then, the femur and tibia were collected, and micro-CT (SkyScan1276, Bruker, Billerica, USA) scanning of tibia and TRAP staining of distal femur were performed. All experiments involving animals were conducted in accordance with the National Institutes of Health guide for the care and use of Laboratory animals (NIH Publications No. 8023, revised 1978). The experimental schemes were approved by the Ethics Review Board of the Affiliated Suqian First People's Hospital of Nanjing Medical University (20220017).

Statistical analysis

All experiments were performed for at least three times. Data are presented as means ± standard deviation (SD). Statistical differences were analyzed by paired-samples *T*-Test, One-way ANOVA, followed by post hoc Bonferroni test (SPSS version 20.0). Values of $p < 0.05$ were considered statistically significant.

RESULTS

USP25 was downregulated in OVX mice and PMOP patients

To carify the expression of USP25 in OVX mice, 8-week-old female C57BL/6 mice were selected to establish OVX model and generate sham group, with 6 mice in each group. At 8 weeks after surgery, proximal femurs of left hind limbs from OVX and sham mice were dissected for the detection of USP25 mRNA expression by qPCR. The right proximal femurs of mice were removed and promptly submerged in liquid nitrogen. Afterwards, the total proteins were extracted and analyzed via Western blot to assess the expression of USP25 protein. The data indicated that the expression of USP25 mRNA and protein in the femurs of sham group was markedly higher than the OVX mice (Fig. 1A–C). Furthermore, the IHC results also demonstrated a significant decrease in the expression of USP25 in OVX mice compared to the sham mice (Fig. 1D,E). We wondered whether the expression of USP25 in the femurs of PMOP patients also decreased apparently at the protein level. The bone tissues of femoral neck from postmenopausal female patients who suffer from traumatic femoral neck fracture and undergo THA (5 in each group) were obtained and detected by Western blot. Compared to the control group, the PMOP group exhibited remarkable low expression of USP25 protein as evident through Western blot (Fig. 1F,G). These results implied that USP25 mRNA and protein were downregulated in both OVX mice and PMOP patients.

USP25 suppressed osteoclastogenesis *in vitro*

Notwithstanding, it has been proved that USP25 could regulate the polarization of RAW264.7 cells and the release of inflammatory cytokines from BMDMs in

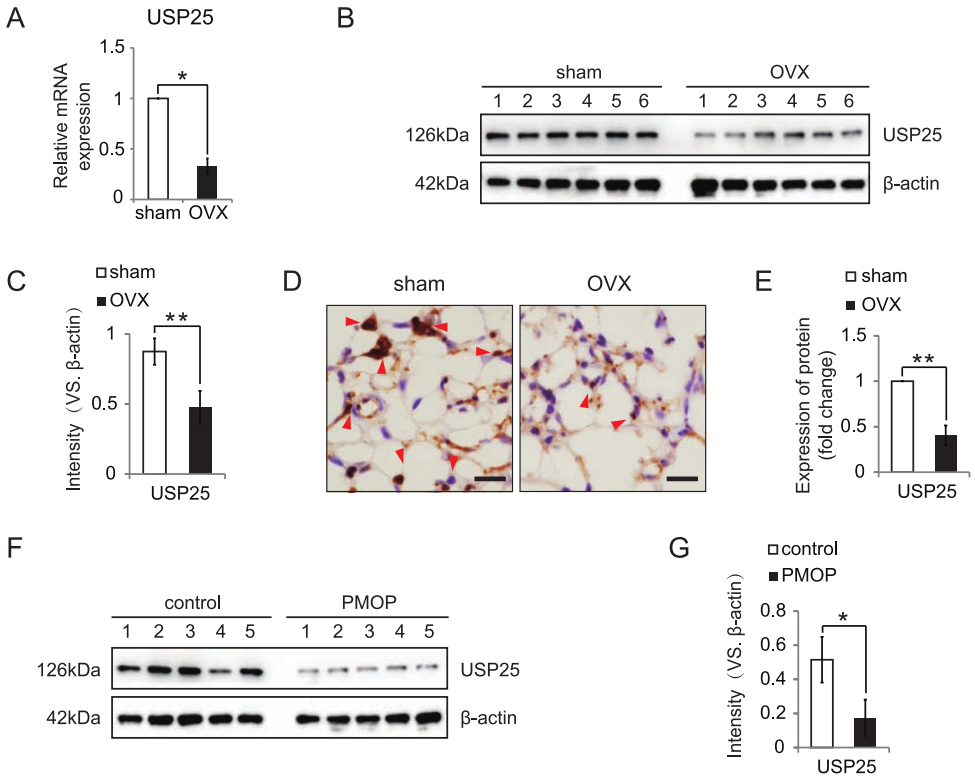

Fig. 1 USP25 was downregulated in OVX mice and PMOP patients. (A) Total mRNA was extracted from the proximal femur of mice, and the relative expression of *usp25* mRNA was detected. *β-actin* mRNA was used as internal control ($n = 6$). (B) Western blot results validating the downregulation of USP25 in the proximal femur of OVX mice ($n = 6$) with quantification (C). Representative IHC micrographs (D) and corresponding quantification (E) of USP25 in the proximal femur of mice. Red arrows indicated the positive expressions ($n = 6$). Western blot (F) and quantitative analysis (G) of protein levels of USP25 in the proximal femur of PMOP patients and women with normal bone mass ($n = 5$). Scale bars were 20 μm. Data are expressed as means ± standard deviation (SD); * $p < 0.05$; ** $p < 0.01$. Experiments were repeated at least 3 times, and similar results were obtained.

inflammation [14, 15], its particular role in osteoclastogenesis remains unknown. For further exploration, RAW264.7 cells were infected with murine USP25-shRNA lentivirus for USP25 gene silencing. Meanwhile, RAW264.7 cells with scr-shRNA were used as a negative control. Under the stimulation of RANKL, knockdown of USP25 led to a significant increase in the number and area of osteoclasts (Fig. 2A,C). To further determine the role of USP25 in osteoclast differentiation, primary BMMs were isolated from the femur and tibia of mice and infected with the indicated lentivirus. After incubating with M-CSF and RANKL for 3 days, the TRAP staining assay was performed. As expected, knockdown of USP25 also promoted the differentiation of primary mouse BMMs into osteoclasts (Fig. 2B,D). For reverse validation, USP25-OE cells were generated with overexpressed lentivirus. The data demonstrated that USP25 overexpression noticeably suppressed osteoclast formation in both RAW264.7 cells (Fig. 2E,G) and BMMs (Fig. 2F,H). Taken together, these results revealed that USP25 indeed suppressed osteoclastogenesis *in vitro*.

USP25 inhibited bone resorption and the expression of osteoclast-related genes

The most important biological function of osteoclast is the ability to resorb bone. We wondered whether the bone resorption function of osteoclasts, in a manner, was also regulated by USP25. Subsequently, RAW264.7 cells and BMMs were seeded in Corning Osteo Assay Surface Plate, and treated with M-CSF and RANKL for 7 days (Fig. 3A). The quantitative analysis results of the bone resorption area indicated that knockdown of USP25 enormously boosted the bone resorption ability of osteoclasts, while USP25 overexpression apparently inhibited the ability (Fig. 3B,C).

Furthermore, the expression levels of osteoclast-related genes: *nfatc1*, *acp5*, and *ctsk* were analyzed by qPCR. Obviously, USP25 overexpression dramatically reduced the expression level of *acp5*, *nfatc1*, and *ctsk* both in RAW264.7 cells and BMMs (Fig. 3D,E). However, knockdown of USP25 distinctly increased the expression level of *acp5*, *nfatc1*, and *ctsk* (Fig. 3D,E), implying that USP25 could downregulate the expres-

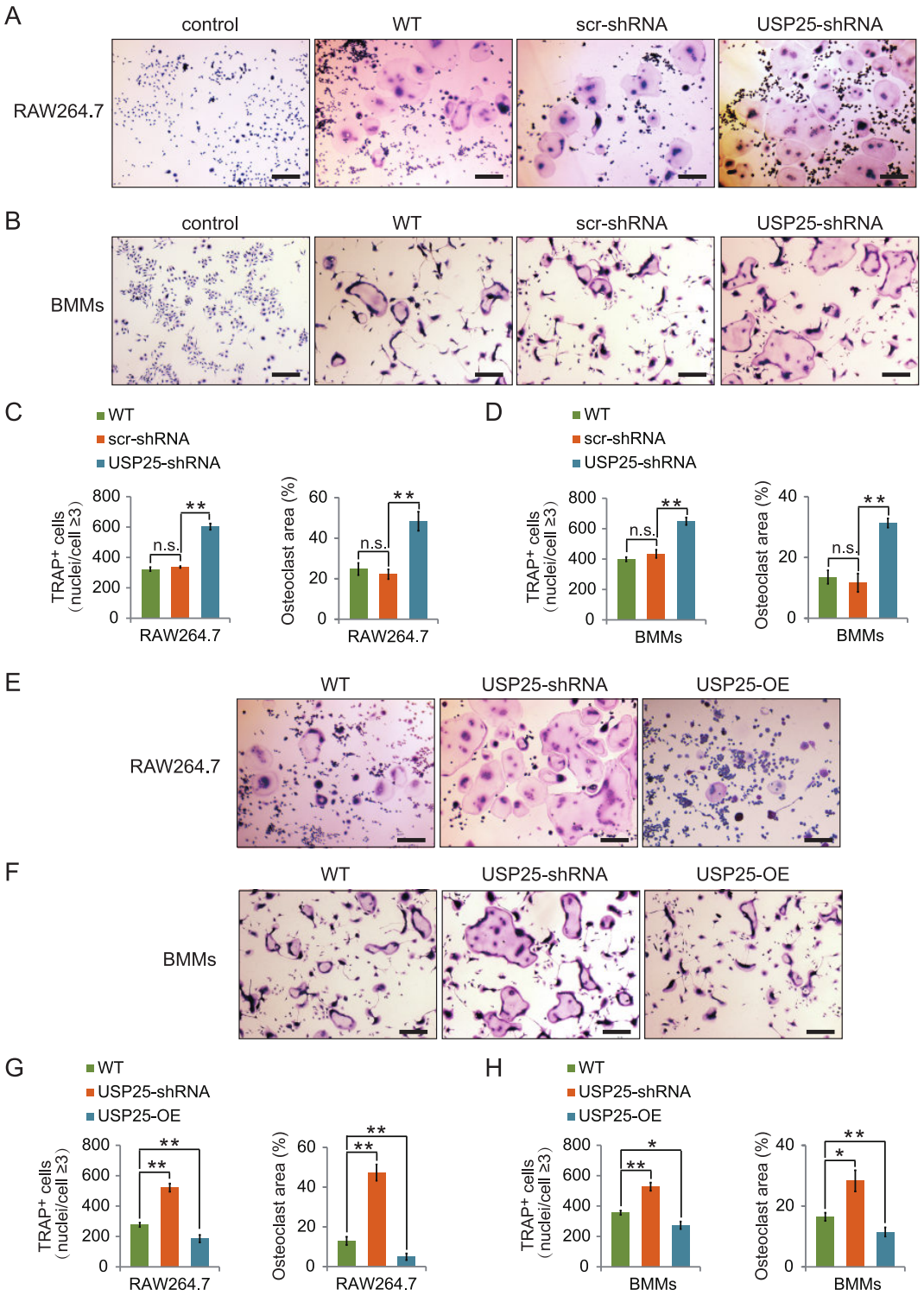

Fig. 2 USP25 suppressed osteoclastogenesis *in vitro*. Cells were infected with murine USP25-shRNA lentivirus for *USP25* gene silencing. Meanwhile, cells with scr-shRNA were used as a negative control. Representative TRAP staining images of RAW264.7 cells (A) and BMMs (B) cultured with RANKL (50 ng/ml) or RANKL (50 ng/ml) and M-CSF (30 ng/ml) for 3 days ($n = 3$). Quantitative analysis of the number and the area of osteoclasts (C, D). Representative TRAP staining images of RAW264.7 cells (E) and BMMs (F) infected with overexpressed lentivirus ($n = 3$). The osteoclast numbers were counted, and the osteoclast area was analyzed (G, H). Scale bars, 100 µm. Data are expressed as means ± standard deviation (SD); * $p < 0.05$, ** $p < 0.01$; n.s., not significant. Experiments were repeated 3 times, and similar results were obtained.

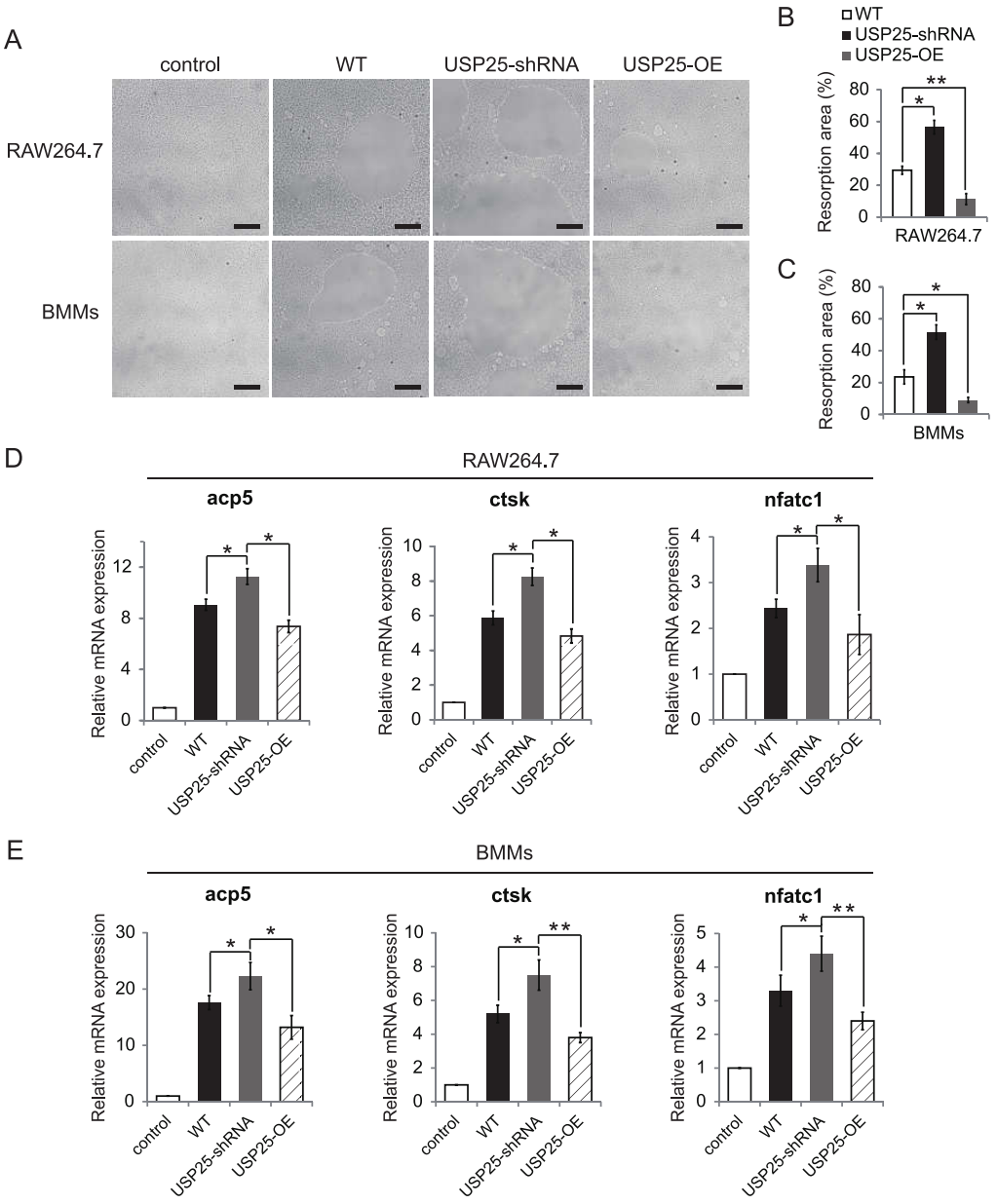

Fig. 3 USP25 inhibited bone resorption and the expression of osteoclast-related genes. Representative images (A) and analysis of bone resorption by osteoclasts cultured on day 7 derived from RAW264.7 cells (B) and BMMs (C) ($n = 3$). Scale bars were 100 μm. Under RANKL (50 ng/ml) or M-CSF (30 ng/ml) and RANKL (50 ng/ml) stimulation for 5 days, total mRNA was respectively isolated from RAW264.7 cells (D) and BMMs (E). Relative expression of *nfatc1*, *acp5*, and *ctsk* mRNA were detected. *β-actin* mRNA was used as internal control ($n = 3$). Data are expressed as means ± standard deviation (SD); * $p < 0.05$; ** $p < 0.01$. Experiments were repeated 3 times, and similar results were obtained.

sion level of genes related to osteoclast.

USP25 regulated osteoclastogenesis by promoting TRAF6 deubiquitination

It has been verified that NF-κB signaling pathway activated by RANKL/RANK plays a vital positive role in osteoclastogenesis [25]. To investigate the mechanism of USP25 in suppressing osteoclast formation, RAW264.7 cells were stimulated with RANKL for 2 days, followed by Western blot analysis. The results indicated that USP25 knockdown increased the expression of NFATc1, while USP25 overexpression decreased the expression of NFATc1 protein (Fig. 4A,C). Furthermore, USP25 overexpression was positively correlated with the protein level of TRAF6. However, it was unexpected that TRAF6 high expression didn't promote

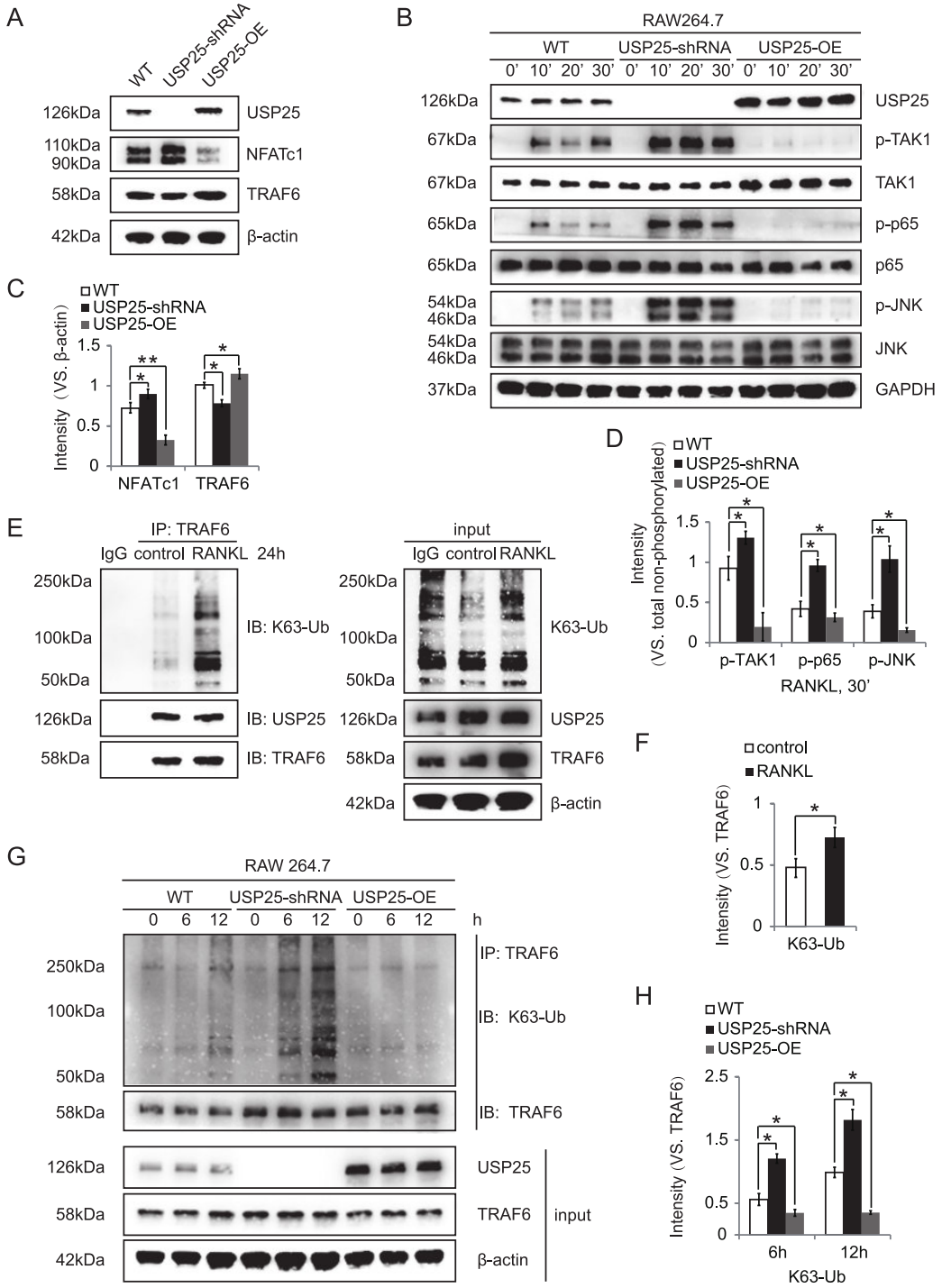

Fig. 4 USP25 regulated osteoclastogenesis by promoting TRAF6 deubiquitination. RAW264.7 cells were stimulated with RANKL (50 ng/ml) for 2 days (A) or the indicated times (B), and Western blot was used to examine the listed proteins, followed by quantitative analysis (C, D) ($n = 3$). Cells were treated with RANKL (50 ng/ml) for 24 h. The TRAF6/K63-Ub/USP25 interaction was examined by Co-IP (E, F) ($n = 3$). Cells were infected with lentivirus, and then stimulated with RANKL (50 ng/ml) for applied time. The cell lysates were immunoprecipitated with anti-TRAF6. The immunoprecipitates were analyzed by Western blot with the indicated antibodies (G), followed by quantitative analysis (H) ($n = 3$). Results are expressed as means ± standard deviation (SD); * $p < 0.05$; ** $p < 0.01$. Experiments were repeated 3 times, and similar results were obtained.

the expression of NFATc1 (Fig. 4A,C). Unambiguously, binding of RANKL to RANK induces the recruitment of TRAF6, and the connection of TRAF6, K63-Ub, and TAB2 (or TAB3), which in turn triggers the degradation of TAB2 (or TAB3), and then promotes the activation of TAK1 [20, 21]. Given that USP25 shows the activity of hydrolyzing K63-Ub [26], we speculated that USP25 might ultimately regulate the expression of NFATc1 by inhibiting the ubiquitin-protein ligase function of TRAF6. To determine the underlying molecular mechanism, we continued to perform Western blot to analyze the expression levels of cytokines located downstream of TRAF6. Intriguingly, USP25 overexpression evidently downregulated the protein levels of p-TAK1, p-p65, and p-JNK (Fig. 4B,D).

Moreover, we further verified the interaction between USP25 and TRAF6 by Co-IP. It was confirmed that USP25 was combined with TRAF6 in RAW264.7 cells, and the stimulation of RANKL significantly increased polyubiquitinated TRAF6 levels (Fig. 4E,F). Polyubiquitinated TRAF6 is able to bind K63-Ub to TAK1 complexes, which is a prerequisite for TAK1 activation [21, 27]. Besides, further investigation indicated that RANKL-induced TRAF6 immunoprecipitation with K63-Ub was blocked by USP25 overexpression and boosted by USP25 knockdown (Fig. 4G,H). Together, our results demonstrated that USP25 might regulate osteoclastogenesis by promoting TRAF6 deubiquitination.

AZ1 exacerbated pathological bone loss in OVX mice

To evaluate the impacts of USP25 inhibition on osteoclastic bone resorption *in vivo*, OVX mice models characterized by pathological bone loss were established. Given that AZ1 showed strong inhibitory activity against USP25, OVX mice were intraperitoneally injected with AZ1 (20 mg/kg in 0.5 ml PBS) or PBS (0.5 ml) daily for 6 weeks, starting from 2 weeks after surgery. To measure the expression of USP25 and TRAF6 proteins, the proximal femur of mice was excised from the right hind limb, and the total proteins were isolated. As anticipated, the results showed that the expression of USP25 protein in PBS group and AZ1 group was notably reduced compared to sham group (Fig. 5A). Following AZ1 administration, the expression of TRAF6 protein in the proximal femur of mice significantly decreased, yet remained higher than that in sham group (Fig. 5A). It could be attributed to AZ1's inhibition of USP25-mediated deubiquitination of TRAF6. We subsequently performed TRAP staining assay, and observed a significant surge in the number of osteoclasts in the distal femoral sections of mice injected with AZ1, as compared to those administered PBS (Fig. 5B). To determine the effects of USP25 on pathological bone loss, the mice tibias were resected and subjected to micro-CT scanning. Apparently, compared to PBS group, AZ1 group exhibited lower bone mass (Fig. 5C,D). These findings suggested that AZ1, which could inhibit USP25 activity, exacerbated the bone destruction in OVX mice.

DISCUSSION

USP25, a deubiquitinase, is associated with inflammation, cancer, and immune response [28, 29]. USP25 could prevent DNA damage and inflammation induced by house dust mites and promote endotoxin tolerance [30, 31]. Meanwhile, it has been proved that USP25 could promote the occurrence of colon cancer and breast cancer [32]. At present, there are few reports on the role of USP25 in regulating bone metabolism. This study revealed a new role of USP25 in regulating osteoclast differentiation in the pathogenesis of PMOP. Moreover, we found that pharmacological inhibition of USP25 exacerbated pathological bone loss in OVX mice, implying that USP25 promotion might be an effective strategy for alleviating PMOP. A study based on bioinformatics analysis has shown that compared to high-BMD samples, USP25 expression was higher in peripheral blood mononuclear cells (PBMCs) from premenopausal low-BMD samples but not in the postmenopausal samples [33]. Herein, we conducted qPCR and Western blot using mouse and human proximal femoral bone tissues to analyze the expression of USP25 gene and protein. The data described that USP25 mRNA and protein were both downregulated in OVX mice and PMOP patients (Fig. 1A–G). We speculated that in order to resist pathological bone loss, the internal compensatory mechanisms of premenopausal OP patients promoted the expression of USP25 in PBMCs.

Some studies proved that USP25 could promote RAW264.7 cells to polarize into M1-like macrophages by USP25-PKM2-glycolysis axis in ischemia reperfusion-induced acute kidney injury [34]. USP25 knockdown enhanced LPS-induced RAW264.7 cells activation [35]. Nevertheless, we confirmed that USP25 could hinder RAW264.7 cells and BMMs from differentiating into osteoclasts *in vitro* (Fig. 2E–H), and it also could suppress the bone resorption function of osteoclasts (Fig. 3A–C).

Furthermore, the underlying molecular mechanism were also investigated. Our qPCR results showed that USP25 could downregulate the expression level of genes related to osteoclast, such as *acp5*, *nfatc1*, and *ctsk* (Fig. 3D,E). Since the NF-κB signaling activated by RANKL/RANK plays a dominant role in osteoclastogenesis [36], Western blot analyses were performed to analyze the expression level of TRAF6, p-TAK1, p-p65 and NFATc1. Interestingly, we found that USP25 overexpression triggered a visible increase in the expression of TRAF6, while the expression of p-TAK1, p-p65 and NFATc1 were downregulated (Fig. 4A–D). We further analyzed the MEK-MAPK pathway and identified that the expression of p-JNK was also reduced (Fig. 4B,D). Considering that TRAF6 was located upstream of these

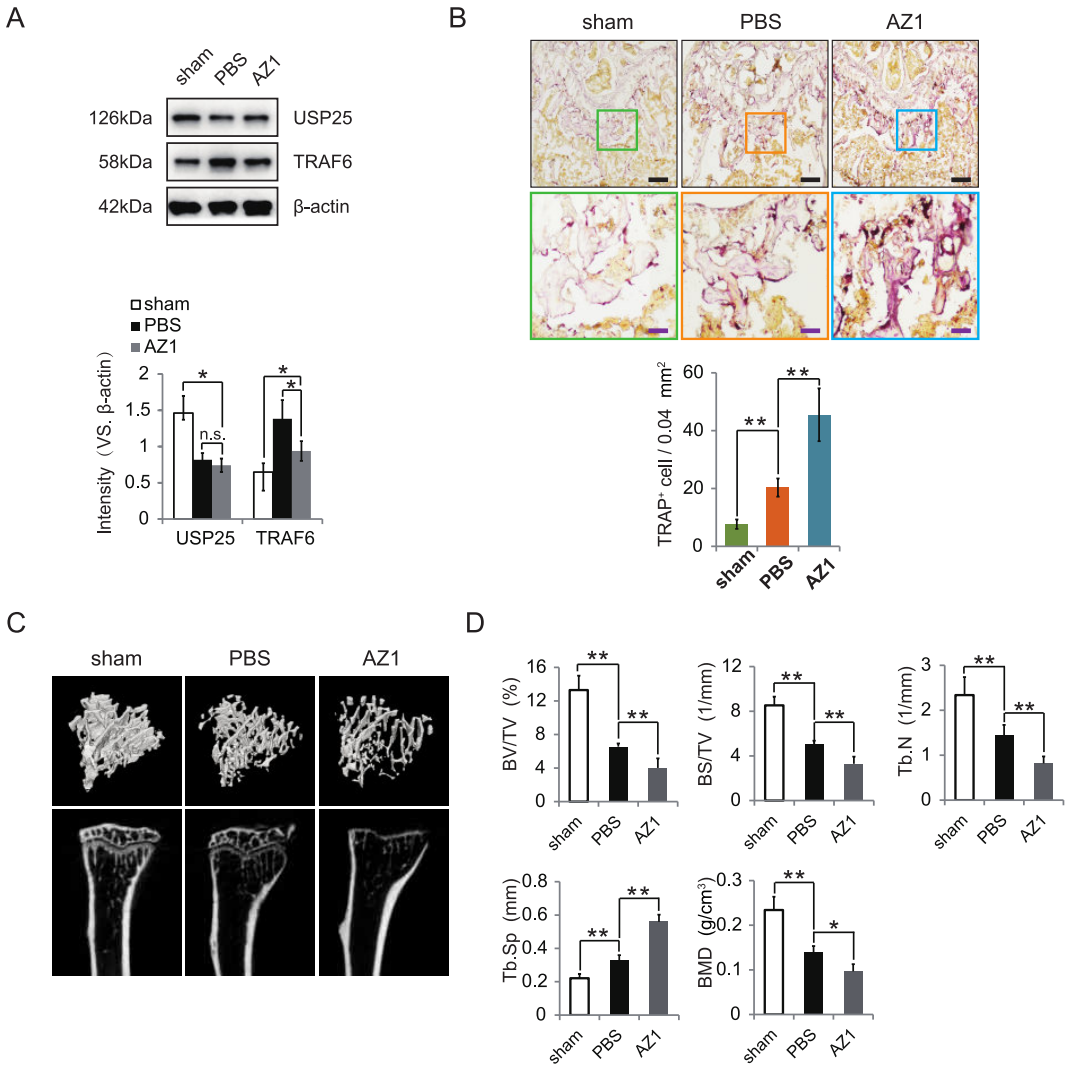

Fig. 5 AZ1 exacerbated pathological bone loss in OVX mice. (A) Western blot was used to detect the listed proteins extracted from the proximal femur of mice, followed by quantitative analysis ($n = 6$). (B) Representative TRAP staining images of femur sections from mice and quantification of osteoclast number ($n = 6$). Scale bars were 100 μm and 25 μm. (C) Representative micro-CT images of mice tibia ($n = 6$). (D) The parameters of micro-CT scanning (BV/TV, BS/TV, Tb.N, Tb.Sp and BMD) of the tibial bones ($n = 6$). All data are shown as means ± standard deviation (SD); * $p < 0.05$, ** $p < 0.01$; n.s., not significant.

cytokines, it was reasonable to assume that there may be an interaction between USP25 and TRAF6. Previous literature has described that TRAF6, a RING-type E3, which could facilitate the binding between K63-Ub and TAB2 (or TAB3), caused the degradation of TAB2 (or TAB3), and thereby promoted the phosphorylation of TAK1 [20, 21]. USP25 negatively regulated IL-17 activated neuroinflammation and NF-κB signaling by isolating K63-Ub from TRAF6 and TRAF5 [37]. The activation of NF-κB signaling and IRF3 were enhanced by USP25 through deubiquitination and stabilizing TRAF6 and TRAF3 in virus infection [38]. Herein, we found that USP25 could restrain TRAF6 polyubiquitination in RAW264.7 cells (Fig. 4G,H), which might be the principal reason why USP25 could inhibit the NF-κB and MAPK pathway induced by RANKL/RANK. Coincidentally, USP25 has been shown to inhibit advanced glycation end-products (AGEs)-induced NF-κB and MAPK signaling through inhibiting the K63 polyubiquitination of TRAF6 in diabetic kidney disease [39].

In addition, AZ1, a small molecule that potently inhibits the enzymatic activity of USP25, has been widely used in *in vivo* studies on USP25 [40, 41]. Here, the results depicted that AZ1 administration resulted in an increase of osteoclast formation, and further accelerated bone loss in mice with OVX-induced osteoporosis (Fig. 5B–D), implying an inhibitory effect of USP25 on osteoclast differentiation and pathological

bone destruction in OVX mice. Currently, due to USP25 and USP28 being homologous proteins with highly similar sequences and structures, most inhibitors have inhibitory effects on both with low specificity. AZ1 can also effectively inhibit the enzymatic activity of USP28. However, there is still a lack of research on USP28 regulating bone homeostasis.

These results indicate that USP25 has the potential to serve as a new target for treating bone loss in PMOP. However, USP25 has a bidirectional immune regulatory effect. To avoid systemic immune effects, tissue-specific targeting strategies are more recommended than systemic interventions. Furthermore, further research is needed to confirm whether USP25 has a regulatory effect on osteogenesis.

CONCLUSION

In conclusion, this is the first study to illuminate that USP25 suppresses osteoclastogenesis and impedes bone resorption by restraining TRAF6 polyubiquitination. USP25 inhibition could dramatically exacerbate pathological bone loss in OVX mice. USP25 may be used as a new target for the treatment of bone loss in PMOP.

Acknowledgements: This study was supported by the Suqian Sci&Tech Program (Grant No. K202146), the Suqian Chinese Medicine Science and Technology Project (Grant No. YB202211), and the Jiangsu Provincial Health Commission Medical Research Project (Grant No. 2023-152).

REFERENCES

1. Liu H, Song P, Zhang H, Zhou F, Ji N, Wang M, Zhou G, Han R, et al (2024) Synthetic biology-based bacterial extracellular vesicles displaying BMP-2 and CXCR4 to ameliorate osteoporosis. *J Extracell Vesicles* **13**, e12429.
2. Rohatgi N, Zou W, Li Y, Cho K, Collins PL, Tycksen E, Pandey G, DeSelm CJ, et al (2023) BAP1 promotes osteoclast function by metabolic reprogramming. *Nat Commun* **14**, 5923.
3. Chang Z, Chen D, Peng J, Liu R, Li B, Kang J, Guo L, Hou R, et al (2024) Bone-targeted supramolecular nanoagonist assembled by accurate ratiometric herbal-derived therapeutics for osteoporosis reversal. *Nano Lett* **24**, 5154–5164.
4. Cui Y, Lv B, Li Z, Ma C, Gui Z, Geng Y, Liu G, Sang L, et al (2023) Bone-targeted biomimetic nanogels re-establish osteoblast/osteoclast balance to treat postmenopausal osteoporosis. *Small* **20**, e2303494.
5. Walker MD, Shane E (2023) Postmenopausal osteoporosis. *N Engl J Med* **389**, 1979–1991.
6. Foessl I, Dimai HP, Obermayer-Pietsch B (2023) Long-term and sequential treatment for osteoporosis. *Nat Rev Endocrinol* **19**, 520–533.
7. Lin W, Hu S, Li K, Shi Y, Pan C, Xu Z, Li D, Wang H, et al (2023) Breaking osteoclast-acid vicious cycle to rescue osteoporosis via an acid responsive organic framework-based neutralizing and gene editing platform. *Small* **20**, e2307595.
8. Luza S, Opazo CM, Bousman CA, Pantelis C, Bush AI, Everall IP (2020) The ubiquitin proteasome system and schizophrenia. *Lancet Psychiatry* **7**, 528–537.
9. Guo Y, Wang M, Zhang S, Wu Y, Zhou C, Zheng R, Shao B, Wang Y, et al (2018) Ubiquitin-specific protease USP34 controls osteogenic differentiation and bone formation by regulating BMP2 signaling. *EMBO J* **37**, e99398.
10. Ullah K, Zubia E, Narayan M, Yang J, Xu G (2018) Diverse roles of the E2/E3 hybrid enzyme UBE2O in the regulation of protein ubiquitination, cellular functions, and disease onset. *FEBS J* **286**, 2018–2034.
11. Shibata N, Ohoka N, Tsuji G, Demizu Y, Miyawaza K, Ui-Tei K, Akiyama T, Naito M (2020) Deubiquitylase USP25 prevents degradation of BCR-ABL protein and ensures proliferation of Ph-positive leukemia cells. *Oncogene* **39**, 3867–3878.
12. Liu B, Sureda-Gómez M, Zhen Y, Amador V, Reverter D (2018) A quaternary tetramer assembly inhibits the deubiquitinating activity of USP25. *Nat Commun* **9**, 4973.
13. Jiang P, Jing Y, Zhao S, Lan C, Yang L, Dai X, Luo L, Cai S, et al (2024) Expression of USP25 associates with fibrosis, inflammation and metabolism changes in IgG4-related disease. *Nat Commun* **15**, 2627.
14. Liu X, Luo W, Chen J, Hu C, Mutsinze RN, Wang X, Zhang Y, Huang L, et al (2022) USP25 deficiency exacerbates acute pancreatitis via up-regulating TBK1–NF-κB signaling in macrophages. *Cell Mol Gastroenterol Hepatol* **14**, 1103–1122.
15. Yang Y, Zhan X, Zhang C, Shi J, Wu J, Deng X, Hong Y, Li Q, et al (2023) USP25-PKM2-glycolysis axis contributes to ischemia reperfusion-induced acute kidney injury by promoting M1-like macrophage polarization and proinflammatory response. *Clin Immunol* **251**, 109279.
16. Zheng Q, Li G, Wang S, Zhou Y, Liu K, Gao Y, Zhou Y, Zheng L, et al (2021) Trisomy 21-induced dysregulation of microglial homeostasis in Alzheimer's brains is mediated by USP25. *Sci Adv* **7**, eabe1340.
17. Patzke JV, Sauer F, Nair RK, Endres E, Proschak E, Hernandez-Olmos V, Sotriffer C, Kisker C (2024) Structural basis for the bi-specificity of USP25 and USP28 inhibitors. *EMBO Rep* **25**, 2950–2973.
18. Kondegowda NG, Filipowska J, Do JS, Leon-Rivera N, Li R, Hampton R, Ogyaadu S, Levister C, et al (2023) RANKL/RANK is required for cytokine-induced beta cell death; osteoprotegerin, a RANKL inhibitor, reverses rodent type 1 diabetes. *Sci Adv* **9**, eadf5238.
19. Yin Q, Lin SC, Lamothe B, Lu M, Lo YC, Hura G, Zheng L, Rich RL, et al (2009) E2 interaction and dimerization in the crystal structure of TRAF6. *Nat Struct Mol Biol* **16**, 658–666.
20. Deng L, Wang C, Spencer E, Yang L, Braun A, You J, Slaughter C, Pickart C, et al (2000) Activation of the IkappaB kinase complex by TRAF6 requires a dimeric ubiquitin-conjugating enzyme complex and a unique polyubiquitin chain. *Cell* **103**, 351–361.
21. Strickson S, Emmerich CH, Goh ETH, Zhang J, Kelsall IR, Macartney T, Hastie CJ, Knebel A, et al (2017) Roles of the TRAF6 and Pellino E3 ligases in MyD88 and RANKL signaling. *Proc Natl Acad Sci USA* **114**, 3481–3489.
22. Fu TM, Shen C, Li Q, Zhang P, Wu H (2018) Mechanism of ubiquitin transfer promoted by TRAF6. *Proc Natl Acad Sci USA* **115**, 1783–1788.

23. Huang C, Zheng Y, Bai J, Shi C, Shi X, Shan H, Zhou X (2021) Hepatocyte growth factor overexpression promotes osteoclastogenesis and exacerbates bone loss in CIA mice. *J Orthop Translat* **27**, 9–16.
24. Zhou Z, Zhang L, Liu Y, Huang C, Xia W, Zhou H, Zhou Z, Zhou X, et al (2022) Luteolin protects chondrocytes from H2O2-induced oxidative injury and attenuates osteoarthritis progression by activating AMPK-Nrf2 signaling. *Oxid Med Cell Longev* **2022**, 5635797.
25. Kim H, Lee K, Kim JM, Kim MY, Kim JR, Lee HW, Chung YW, Shin HI, et al (2021) Selenoprotein W ensures physiological bone remodeling by preventing hyperactivity of osteoclasts. *Nat Commun* **12**, 2258.
26. Li Z, Liu B, Lambertsen KL, Clausen BH, Zhu Z, Du X, Xu Y, Poulsen FR, et al (2023) USP25 inhibits neuroinflammatory responses after cerebral ischemic stroke by deubiquitinating TAB2. *Adv Sci* **10**, e2301641.
27. Jo YJ, Lee HI, Kim N, Hwang D, Lee J, Lee GR, Hong SE, Lee H, et al (2020) Cinchonine inhibits osteoclast differentiation by regulating TAK1 and AKT, and promotes osteogenesis. *J Cell Physiol* **236**, 1854–1865.
28. Liu Z, Qi M, Tian S, Yang Q, Liu J, Wang S, Ji M, Yu R, et al (2022) Ubiquitin-specific protease 25 aggravates acute pancreatitis and acute pancreatitis-related multiple organ injury by destroying tight junctions through activation of the STAT3 pathway. *Front Cell Dev Biol* **9**, 806850.
29. Zhu W, Zheng D, Wang D, Yang L, Zhao C, Huang X (2021) Emerging roles of ubiquitin-specific protease 25 in diseases. *Front Cell Dev Biol* **9**, 698751.
30. Gan C, Wang Y, Zhao Q, Kong M, Chen J, Zhang W, Tan L, Tian M (2022) USP25 inhibits DNA damage by stabilizing BARD1 protein in a house dust mite-induced asthmatic model *in vitro* and *in vivo*. *Cell Biol Int* **46**, 922–932.
31. Wen J, Bai H, Chen N, Zhang W, Zhu X, Li P, Gong J (2019) USP25 promotes endotoxin tolerance via suppressing K48-linked ubiquitination and degradation of TRAF3 in Kupffer cells. *Mol Immunol* **106**, 53–62.
32. Zhou L, Qin B, Yassine DM, Luo M, Liu X, Wang F, Wang Y (2023) Structure and function of the highly homologous deubiquitinases ubiquitin specific peptidase 25 and 28: Insights into their pathophysiological and therapeutic roles. *Biochem Pharmacol* **213**, 115624.
33. Shen J, Fu B, Wu Y, Yang Y, Lin X, Lin H, Liu H, Huang W (2022) USP25 expression in peripheral blood mononuclear cells is associated with bone mineral density in women. *Front Cell Dev Biol* **9**, 811611.
34. Yang Y, Zhan X, Zhang C, Shi J, Wu J, Deng X, Hong Y, Li Q, et al (2023) USP25-PKM2-glycolysis axis contributes to ischemia reperfusion-induced acute kidney injury by promoting M1-like macrophage polarization and proinflammatory response. *Clin Immunol* **251**, 109279.
35. Ding C, Li F, Long Y, Zheng J (2017) Chloroquine attenuates lipopolysaccharide-induced inflammatory responses through upregulation of USP25. *Can J Physiol Pharmacol* **95**, 481–491.
36. Xie G, Huang C, Jiang S, Li H, Gao Y, Zhang T, Zhang Q, Pavel V, et al (2024) Smoking and osteoimmunology: Understanding the interplay between bone metabolism and immune homeostasis. *J Orthop Translat* **46**, 33–45.
37. Zhong B, Liu X, Wang X, Chang SH, Liu X, Wang A, Reynolds JM, Dong C (2012) Negative regulation of IL-17-mediated signaling and inflammation by the ubiquitin-specific protease USP25. *Nat Immunol* **13**, 1110–1117.
38. Lin D, Zhang M, Zhang MX, Ren Y, Jin J, Zhao Q, Pan Z, Wu M, et al (2015) Induction of USP25 by viral infection promotes innate antiviral responses by mediating the stabilization of TRAF3 and TRAF6. *Proc Natl Acad Sci USA* **112**, 11324–11329.
39. Liu B, Miao X, Shen J, Lou L, Chen K, Mei F, Chen M, Su X, et al (2023) USP25 ameliorates diabetic nephropathy by inhibiting TRAF6-mediated inflammatory responses. *Int Immunopharmacol* **124**, 110877.
40. Zheng Q, Song B, Li G, Cai F, Wu M, Zhao Y, Jiang L, Guo T, et al (2022) USP25 inhibition ameliorates Alzheimer's pathology through the regulation of APP processing and Aβ generation. *J Clin Invest* **132**, e152170.
41. Kim DK, Weller B, Lin CW, Sheykhkarimli D, Knapp JJ, Dugied G, Zanzoni A, Pons C, et al (2022) A proteome-scale map of the SARS-CoV-2–human contactome. *Nat Biotechnol* **41**, 140–149.